A human ES/iPS cells → definitive endoderm cells → hepatoblast-like cells (HBCs)

6 days — Activin A (100 ng/ml) + Ad-FOXA2 on day 2 (3,000 VP/cells)

3 days — BMP4 (20 ng/ml) FGF4 (20 ng/ml)

self-replicate on human laminin 111-coated dishes

B

% of Max

AFP — ALB — CK19 — EpCAM

C

ALB-/CK19-/DAPI — ALB-/CK19+/DAPI — ALB+/CK19-/DAPI — ALB+/CK19+/DAPI

20 μm

colony number

ALB-/CK19-   ALB-/CK19+   ALB+/CK19-   ALB+/CK19+

D

ALB

ng/ml

SHAM   HBCs

**Fig. S1   The hepatoblast-like cells (HBCs) generated from hESCs were characterized.**

(**A**) hESCs were differentiated into the HBCs via definitive endoderm cells.   The HBCs were maintained on human LN111.   (**B**) The expression levels of hepatoblast markers (AFP, ALB, CK19, and EpCAM) in the HBCs were examined by FACS

1

analysis. (**C**) Clonal assay of the HBC was performed. The HBCs were plated at a density of 200 cells/cm^2 on human LN111-coated 96-well plates. The colonies were separated into four groups based on the expression of ALB and CK19 (ALB and CK19 double-negative, ALB negative and CK19 positive, ALB positive and CK19 negative, and ALB and CK19 double-positive groups). The numbers represent wells in which the colony was observed in three 96-well plates (total 288 wells). Five days after plating, the cells were fixed with 4% PFA and used for double immunostaining. Nuclei were counterstained with DAPI (blue). (**D**) The HBCs were transplanted into CCl$_4$ (2 mL/kg)-treated Rag2/IL2 receptor gamma double-knockout mice. The human ALB level in recipient mouse serum was measured at 2 weeks after transplantation.

2
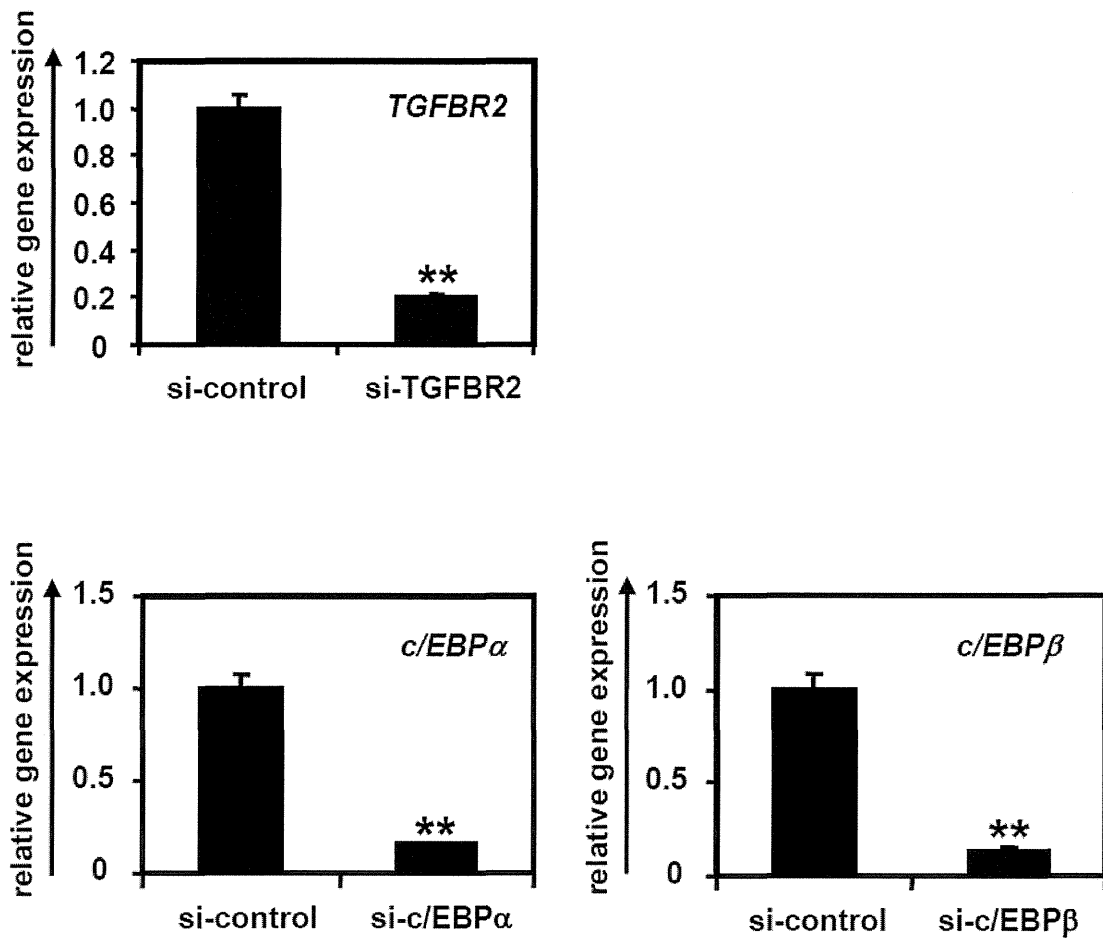
Fig. S2 c/EBPα, c/EBPβ, or TGFBR2 were knocked-down in the HBCs by si-c/EBPα, si-c/EBPβ, or si-TGFBR2 transfection, respectively.

The HBCs were transfected with 50 nM of si-control, si-c/EBPα, si-c/EBPβ, or si-TGFBR2. Two days after transfection, the gene expression levels of *c/EBPα, c/EBPβ,* or *TGFBR2* were examined by real-time RT-PCR in si-c/EBPα-, si-c/EBPβ-, or si-TGFBR2-transfected cells, respectively. On the y axis, the gene expression levels of *c/EBPα, c/EBPβ,* or *TGFBR2* in si-control-transfected cells were taken as 1.0. **$P<0.01$ (compared with the si-control-transfected cells).

3
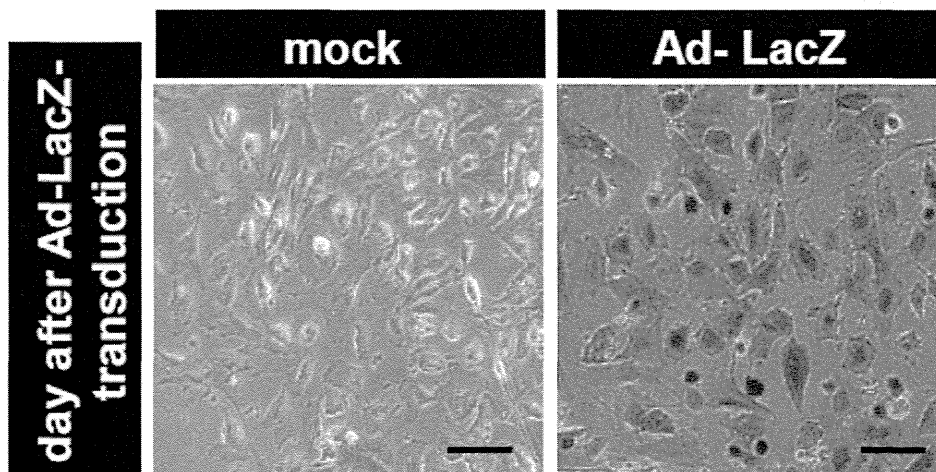
Fig. S3　Ad vectors efficiently transduced the HBCs.

　　The HBCs were transduced with 3,000 VP/cell of Ad-LacZ for 1.5 hr.　The day after transduction, X-gal staining was performed.　The scale bars represent 50 μm.

4
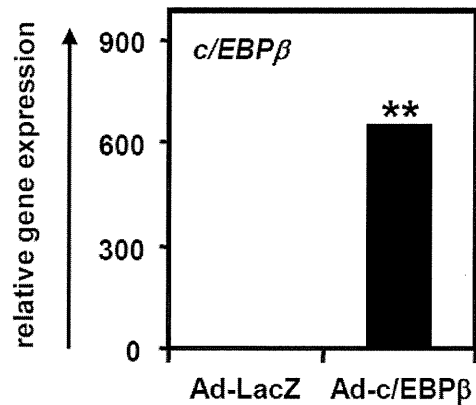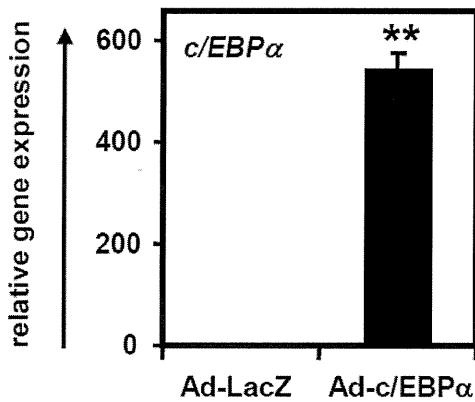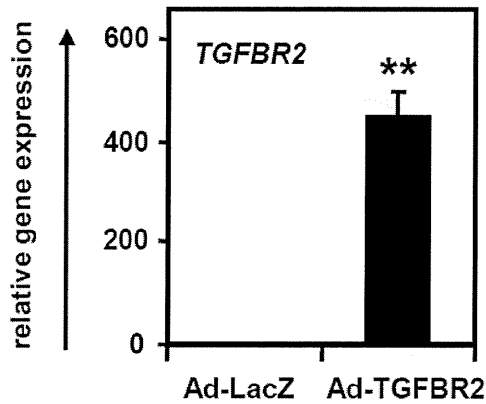
Fig. S4 c/EBPα, c/EBPβ, or TGFBR2 were overexpressed in the HBCs by Ad-c/EBPα, Ad-c/EBPβ, or Ad-TGFBR2 transduction, respectively.

The HBCs were transduced with 3,000 VP/cells of Ad-c/EBPα, Ad-c/EBPβ, or Ad-TGFBR2 for 1.5 hr. Two days after Ad vectors transduction, the gene expression levels of *c/EBPα*, *c/EBPβ*, or *TGFBR2* were examined by real-time RT-PCR in Ad-c/EBPα-, Ad-c/EBPβ-, or Ad-TGFBR2-transduced cells, respectively. On the y axis, the gene expression levels of *c/EBPα*, *c/EBPβ*, or *TGFBR2* in Ad-LacZ-transduced cells were taken as 1.0. **P<0.01 (compared with the Ad-LacZ-transfected cells).

5

- 222 -
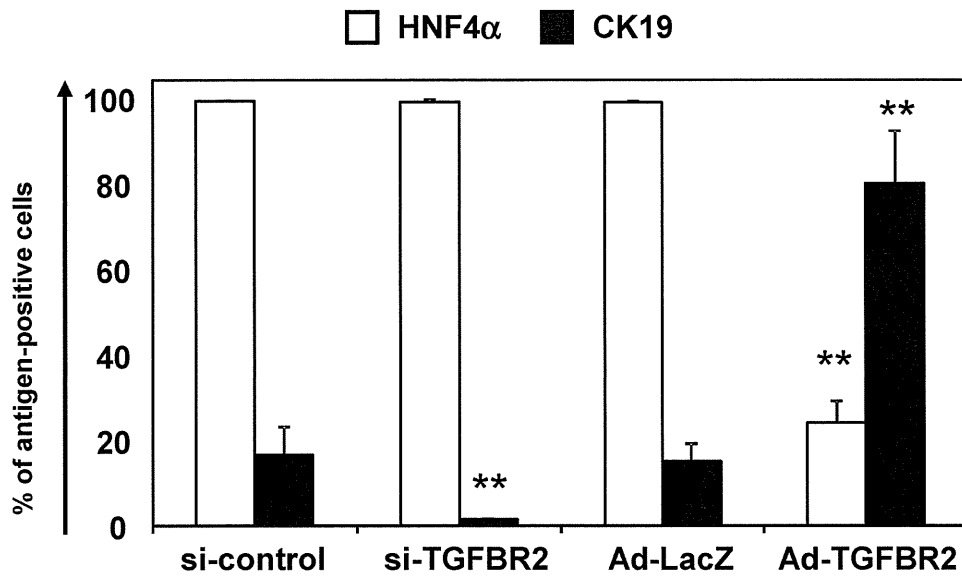
Fig. S5   TGFBR2 overexpression or knockdown in the HBCs promotes cholangiocyte or hepatocyte differentiation, respectively.

The si-control-, si-TGFBR2-, Ad-LacZ- or Ad-TGFBR2-transduced HBCs (total of 1.0×10^6 cells) were transplanted into CCl_4 (2 mL/kg)-treated Rag2/IL2 receptor gamma double knockout mice by intrasplenical injection.   Expressions of HNF4α and CK19 were examined by immunohistochemistry at 2 weeks after transplantation. Semiquantitative analysis of the immunofluorescent staining was performed in the human cell clusters. $*P<0.05$; $**P<0.01$.

6

Fig. S6   c/EBP-binding site on the TGFBR2 promoter region

The consensus sequence of the c/EBP-binding site is described. (http://www.cbil.upenn.edu/cgi-bin/tess/tess).

7
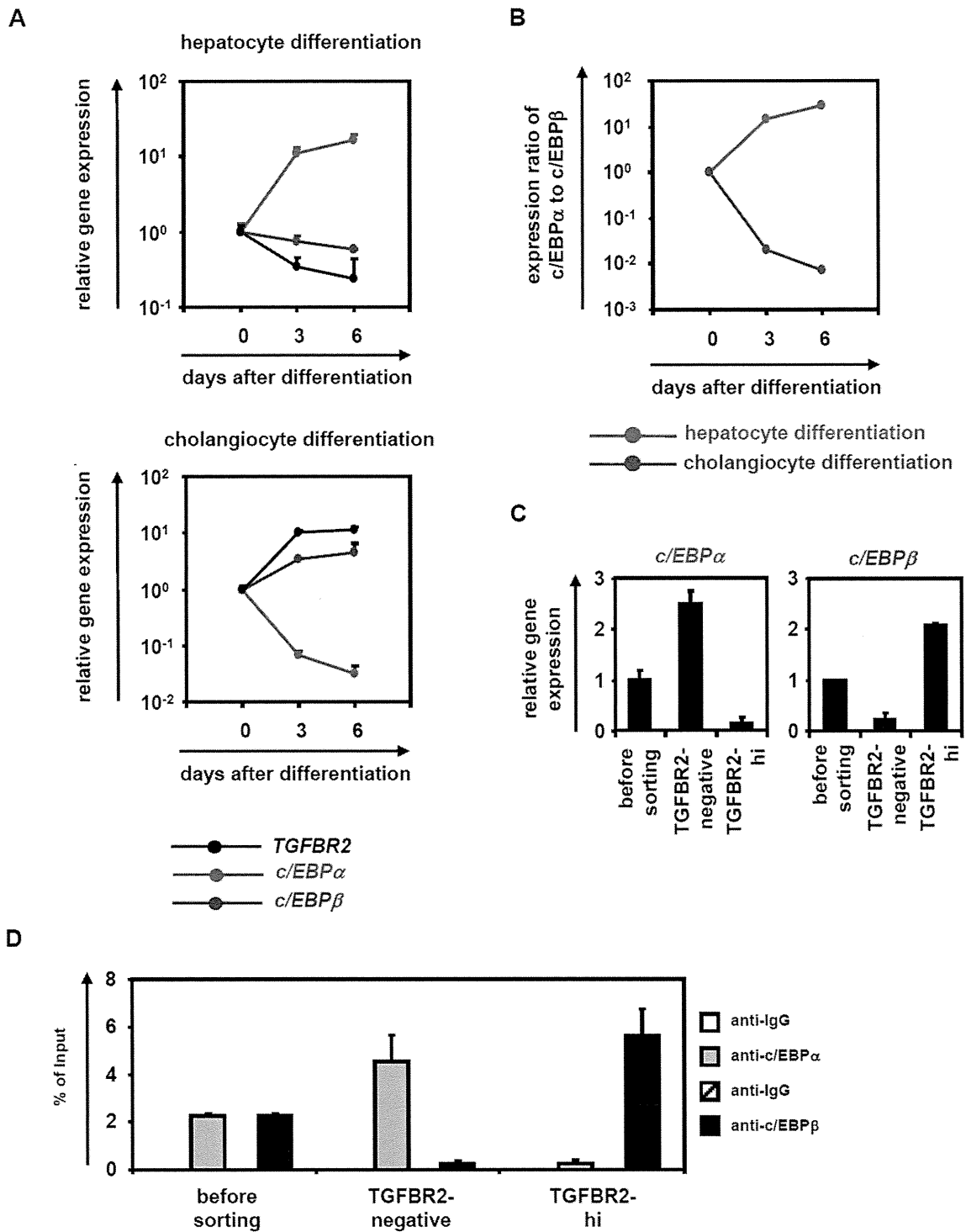
Fig. S7   Temporal gene expression levels of *TGFBR2*, *c/EBPα*, and *c/EBPβ* in hepatocyte and cholangiocyte differentiation.

The HBCs were differentiated into hepatocyte-like cells or cholangiocyte-like cells as shown in figure 1A.   (A) Temporal gene expression levels of *TGFBR2*,

c/EBPα, and *c/EBPβ* in hepatocyte differentiation and cholangiocyte differentiation of the HBCs were examined by real-time RT-PCR. On the y axis, the gene expression levels in the HBCs were taken as 1.0. (**B**) The temporal ratio of c/EBPα to c/EBPβ was demonstrated in hepatocyte and cholangiocyte differentiation. The ratio of c/EBPα to c/EBPβ in the HBCs was taken as 1.0. (C) The HBCs were cultured on Matrigel for 5 days, and then the expression level of TGFBR2 was examined by FACS analysis. TGFBR2-negative, -lo, and –hi populations were collected as described in figure 1F. Real-time RT-PCR analysis was performed in three populations (before sorting, TGFBR-negative, and TGFBR2-hi) to measure the expression levels of *c/EBPα* and *c/EBPβ*. (**D**) The recruitment of c/EBPα or c/EBPβ to the TGFBR2 promoter region in three populations (before sorting, TGFBR-negative, and TGFBR2-hi) was examined by ChIP assay.

9
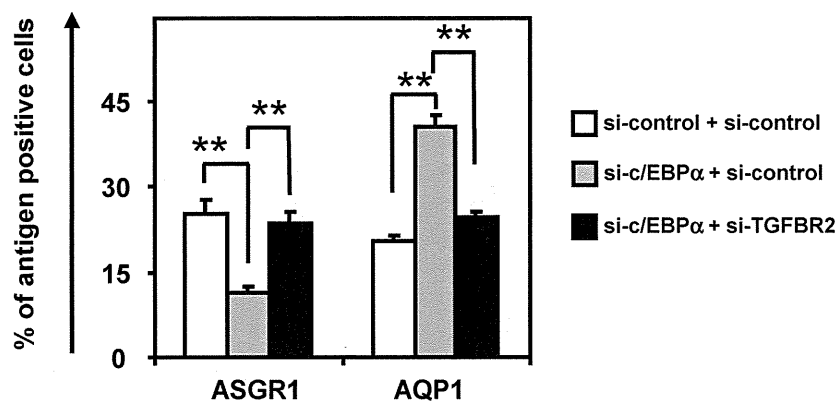
Fig. S8 Inhibition of hepatocyte differentiation by si-c/EBPα transfection was rescued by si-TGFBR2 transfection.

The HBCs were transfected with 50 nM of each of si-control + si-control, si-c/EBPα + si-control, or si-c/EBPα + si-TGFBR2 and cultured with the differentiation hESF-DIF medium for 10 days.   The efficiency of hepatocyte or cholangiocyte differentiation was measured by estimating the percentage of ASGR1- or AQP1-positive cells, respectively, using FACS analysis.   *P<0.05; **P<0.01.

10

Fig. S9 The lineage segregation of hepatoblasts might be explained by c/EBP-mediated control of TGFBR2 expression.

In hepatocyte differentiation from hepatoblasts, c/EBPα promotes hepatocyte differentiation via negative regulation of TGFBR2 expression. On the other hand, c/EBPβ promotes cholangiocyte differentiation via positive regulation of TGFBR2 expression in cholangiocyte differentiation.

11

Supplemental Table 1　The primary antibodies used in this study

Antigen	Species	Company (catalog number)	Dilution
CK19	rabbit	Abcam (ab52625)	1/250
AFP	mouse	Cell Signaling (#3903)	1/100
c/EBPβ	rabbit	Santa Cruz Biotechnology (sc-150AC)	1/50
ALB (ELISA)	goat	Bethyl Laboratories (E80-129)	
ALB (FCM)	rabbit	Abcam (ab135575)	1/40
ALB (IHC)	goat	Santa Cruz Biotechnology (sc-46293)	1/200
c/EBPα	rabbit	Abcam (ab40764)	1/50
HNF4α	abcm	Abcam (ab36175)	1/100
TGFBR2	mouse	Santa Cruz Biotechnology (sc-17799)	1/50
ASGR1	goat	Santa Cruz Biotechnology (sc-13467)	1/50
CYP3A4	goat	Santa Cruz Biotechnology (sc-27639)	1/200
AQP1	mouse	Abcam (ab9566)	1/40
EpCAM	mouse	Militenyi Biotec (130-091-254)	1/50

1

Supplemental Table 2   The secondary antibodies used in this study

Antigen	label	Company	Species	Dilution
rabbit IgG	alexa fluor 488	Molecular Probes	goat	1/1000
rabbit IgG	alexa fluor 488	Molecular Probes	chicken	1/1000
mouse IgG	alexa fluor 488	Molecular Probes	rabbit	1/1000
goat IgG	alexa fluor 488	Molecular Probes	rabbit	1/1000
rabbit IgG	alexa fluor 594	Molecular Probes	mouse	1/1000
goat IgG	alexa fluor 594	Molecular Probes	mouse	1/1000
goat IgG	alexa fluor 594	Molecular Probes	chicken	1/1000
goat IgG	alexa fluor 594	Molecular Probes	donkey	1/1000
mouse IgG	alexa fluor 594	Molecular Probes	chicken	1/1000

2

Supplemental Table 3   The primers used for real-time RT-PCR in this study

Genes	Primers (forward/reverse; 5' to 3')
CK7	AGACGGAGTTGACAGAGCTG/GGATGGCCCGGTTCATCTC
CK19	CTCCCGCGACTACAGCCACT/TCAGCTCATCCAGCACCCTG
HES1	ATGGAGAAAAATTCCTCGTCCC/TTCAGAGCATCCAAAATCAGTGT
SOX9	TTTCCAAGACACAAACATGA/AAAGTCCAGTTTCTCGTTGA
integrin β4	GCAGCTTCCAAATCACAGAGG/CCAGATCATCGGACATGGAGTT
TO	GGCAGCGAAGAAGACAAATC/TCGAACAGAATCCAACTCCC
αAT	ACTGTCAACTTCGGGGACAC/CATGCCTAAACGCTTCATCA
ALB	GCACAGAATCCTTGGTGAACAG/ATGGAAGGTGAATGTTTTCAGCA
TGFBR2	GGAAACTTGACTGCACCGTT/CTGCACATCGTCCTGTGG
c/EBPα	TTCACATTGCACAAGGCACT/GAGGGACCGGAGTTATGACA
c/EBPβ	CGTGTACACACGCGTTCAG/CTCTCTGCTTCTCCCTCTGC
HNF6	CAAACCCTGGAGCAAACTCAA/TGTGTTGCCTCTATCCTTCCC
HNF1β	ACCAAGCCGGTCTTCCATACT/GGTGTGTCATAGTCGTCGCC
CYP2D6	CTTTCGCCCCAACGGTCTC/TTTTGGAAGCGTAGGACCTTG
TTR	TCATCGTCTGCTCCTCCTCT/AGGTGTCATCAGCAGCCTTT
HNF1α	AACACCTCAACAAGGGCACTC/CCCCACTTGAAACGGTTCCT
CYP3A4	AAGTCGCCTCGAAGATACACA/AAGGAGAGAACACTGCTCGTG
mouse αAT	TTGCTCGACACAACATGGAAT/ACGTCCCAGTTTGACATCTCT
mouse CYP7A1	GCTGTGGTAGTGAGCTGTTG/GTTGTCCAAAGGAGGTTCACC
mouse AQP1	AGGCTTCAATTACCCACTGGA/CTTTGGGCCAGAGTAGCGAT
mouse integrin β4	AGAGCTGTACCGAGTGCATC/TGGTGTCGATCTGGGTGTTCT

3

Supplemental Table 4   The primers used for ChIP assay in this study

	Primers (forward/reverse; 5' to 3')
c/EBP binding site A	TCACAACTTTCTAAGTCCCAATTTT/ACTGAGGCAGGGACTGTGTC
c/EBP binding site B	AACTGAAATGTCTTCCTTTTTCAA/CAGGAGGAGTAGAGCCAGCA
c/EBP binding site C	GCCACATTGTGTTTCAGGA/ TTAGCCGAGAATGATGTCACC
c/EBP binding site D	CCAGAGGGCTGTACAGAATCA/ CCAGATTTGCCCAAGACATT
c/EBP binding site E	TGCCTACTGGGTGCTAGAGG/AACCTTCAGAGACAGCGATCA
β-actin	CCGGCGGGGTCTTTGTCTGAGC/GGGCCGGCCGCGTTATTACCA

4

Masahiro Yodoshi
Natsumi Ikeda
Naoko Yamaguchi
Mana Nagata
Noriaki Nishida
Kazuaki Kakehi
Takao Hayakawa
Shigeo Suzuki

Faculty of Pharmaceutical
Sciences, Kinki University,
Kowakae, Higashi-Osaka, Osaka,
Japan

Research Article

A novel condition for capillary electrophoretic analysis of reductively aminated saccharides without removal of excess reagents

We have identified novel CE conditions for the separation of 7-amino-4-methylcoumarin-labeled monosaccharides and oligosaccharides from glycoproteins. Using a neutrally coated capillary and alkaline borate buffer containing hydroxypropylcellulose and ACN, saccharide derivatives form anionic borate complexes, which move from the cathode to the anode in an electric field and are detected near the anodic end. Excess labeling reagents and other fluorescent products remain at the cathodic end. Fluorimetric detection using an LED as a light source enables determination of monosaccharide derivatives with good linearity between at least 0.4 and 400 μM, may correspond to 140 amol to 140 fmol. The lower LOD (S/N = 5) is only 80 nM in the sample solution (ca. 28 amol). The results were comparable to reported values using fluorometric detection LC. The method was also applied to the analysis of oligosaccharides that were enzymatically released from glycoproteins. Fine resolution enables profiling of glycans in glycoproteins. The applicability of the method was examined by applying it to other derivatives labeled with nonacidic tags such as ethyl *p*-aminobenzoate- and 2-aminoacridone-labeled saccharides.

1 Introduction

Most saccharides are neutral, highly hydrophilic, and do not possess chromophoric or fluorometric functions. Various labeling reagents have therefore been developed to improve sensitivity and enhance resolution in LC and CE. Numerous fluorescent amines have been reported for the derivatization of saccharides based on reductive amination. In this labeling reaction, a saccharide is converted to a Schiff's base in the presence of a large excess of an aromatic amine and the resultant imide derivative is converted immediately to a chemically stable 1-amino-1-alditol by reduction with sodium cyanoborohydride. These reactions are well summarized in a number of reviews [1–3]. 8-Aminopyrene-1,3,6-trisulfonic

Correspondence: Dr. Shigeo Suzuki, Faculty of Pharmaceutical Sciences, Kinki University in 3-4-1, Kowakae, Higashi-Osaka, Osaka, Japan
E-mail: suzuki@phar.kindai.ac.jp
Fax: +81-6-6721-2353

Abbreviations: ABEE, ethyl *p*-aminobenzoate; **AMAC,** 2-aminoacridone; **AMC,** 7-amino-4-methylcoumarin; **APTS,** 8-aminopyrene-1,3,6-trisulfonic acid; **BSM,** bovine submaxillary mucin; **Fuc,** fucose; **Gal,** galactose; **GalNAc,** *N*-acetylgalactosamine; **GlcNAc,** *N*-acetylglucosamine; **IS,** internal standard; **Man,** mannose; **ManNAc,** *N*-acetylmannosamine; **NeuAc,** *N*-acetylneuraminic acid; **NeuGc,** *N*-glycolylneuraminic acid; **Rha,** rhamnose; **Xyl,** xylose

acid (APTS) is often used for sensitive detection of glycoprotein glycans in CE analysis because APTS derivatives show intense fluorescence signals under irradiation by an argon ion laser. The negative charge attributable to the three sulfonate groups of APTS moves derivatized saccharides to the anode at high velocity, which enables the rapid analysis of glycoprotein glycans [4–8]. 2-Aminopyridine is often used for identification of glycoprotein-derived oligosaccharides because retention indices for more than several hundred glycans have been accumulated in RP and normal phase LC, as well as anion-exchange LC for sialylated oligosaccharides [9–13]. However, the high hydrophilicity of APTS and 2-aminopyridine hampers solvent extraction of excess reagents. Therefore, tedious steps are required to remove excess reagents from the reaction mixture. Moreover this process may cause partial loss of derivatives, which impairs quantitative analysis.

We previously described a labeling method using 7-amino-4-methylcoumarin (AMC) as a fluorescent probe [14]. AMC-labeled oligosaccharides displayed one- to two-order higher intensities in ESI-MS than derivatives labeled with other reagents. However the method requires two-step SPE for the removal of excess AMC and by-products generated in the course of reaction, which requires tedious procedures and may partially impair quantitative determination.

Colour Online: See the article online to view Fig. 5 in colour.

This work presents selective and sensitive separation conditions for profiling monosaccharides and oligosaccharides found in glycoproteins, without requiring the two-step extractive removal of excess labeling reagent. AMC-labeled saccharides have no charge in alkaline buffer. However in the presence of boric acid, the adjacent hydroxyl groups on saccharides form acidic complexes with borate, which provide a strong negative charge to AMC-labeled saccharides and induces their movement toward the anode. This method allows selective quantification of all of component monosaccharides found in glycoprotein hydrolysates; *N*-acetylglucosamine (GlcNAc), *N*-acetylgalactosamine (GalNAc), galactose (Gal), mannose (Man), fucose (Fuc), *N*-acetylneuraminic acid (NeuAc), and *N*-glycolylneuraminic acid (NeuGc). Application of LED-based fluorescent detection enables subattomole level detection of monosaccharides. This borate-based separation mode was also applied to the selective detection of glycoprotein-derived oligosaccharides.

2 Materials and methods

2.1 Materials

We obtained AMC from Tokyo Kasei Kogyo Co. (Tokyo, Japan). Pyridine-borane, DMF, ethyl *p*-aminobenzoate (ABEE), ACN, methanol, TFA, and glacial acetic acid were obtained from Wako Pure Chemical Industries (Doshomachi, Osaka, Japan). β-*N*-Acetylhexosaminidase (jack bean, EC 3.2.1.52) and β-galactosidase (jack bean, EC 3.2.1.23) were obtained from Seikagaku Kogyo K.K. (Tokyo, Japan). Dimethylamine-borane complex, 2-aminoacridone (AMAC), *N*-acetylneuraminate pyruvate-lyase from *Escherichia coli* K-12, human transferrin, fetal calf serum fetuin, bovine pancreas ribonuclease B, human α_1-acid glycoprotein, bovine submaxillary mucin (BSM), and ovalbumin were obtained from Sigma-Aldrich Japan K.K. (Tokyo, Japan). Neuraminidase from *Arthrobacter ureafaciens* and saccharide specimens were obtained from Nacalai Tesque (Kyoto, Japan). Peptide-N^4-(acetyl-β-glucosaminyl)-asparagine amidase F (EC 3.5.1.52) was purchased from F. Hoffmann-La Roche (Mannheim, Germany). Isomaltooligosaccharides were obtained through partial hydrolysis of dextran (100 mg) with 1 mL of 0.1 M hydrochloric acid for 4 h at 100°C; the lyophilized powder was used as a glucose ladder. Water was purified using a Milli-Q device (Millipore, Milford, MA, USA). Other reagents and solvents were of the highest commercially available grade. In addition, SCX-type SPE cartridges (100 mg) and OASIS HLB cartridges (10 mg) were obtained from Silicycle (Quebec, Canada) and Nihon Waters K.K. (Tokyo, Japan), respectively. Graphitized carbon was from Alltech Japan (Tokyo, Japan). AMC-labeled maltose was prepared as described in a previous report, and AMC-labeled oligosaccharides derived from glycoprotein specimens were fractionated by HPLC and used for peak identifications [14].

2.2 Hydrolysis of glycoprotein specimens

Hydrolysis of glycoprotein specimens was carried out as previously described [15]. Two portions of a solution of glycoprotein specimen (0.1 mg each) were lyophilized in glass tubes (4 mm id, 12 cm long). For the analysis of component neutral aldoses, one of the sample residues was dissolved in 100 μL of 2 M TFA and the tube was sealed after exchanging air in the tube with nitrogen three times using a vacuum desiccator connected to nitrogen and vacuum lines, and the tube was then sealed and heated for 6 h at 100°C. The resultant solution was mixed with 20 μL of 0.1 mM rhamnose (Rha, 2 nmol) as internal standard (IS), and the residue was lyopilized to dryness for derivatization with AMC. For the analysis of hexosamines, a sample was dissolved in 100 μL of 4 M HCl and the solution was heated for 6 h at 100°C under a nitrogen atmosphere. The solution was then evaporated to dryness, followed by addition of 2 nmol IS. Acetamide groups were hydrolyzed in this process. Therefore the residue was dissolved in 250 μL of a saturated solution of sodium bicarbonate and the solution mixed with 50 μL of acetic anhydride under vigorous shaking for 30 min and stored in a refrigerator overnight. The reaction mixture was mixed with 500 μL of water and DI by passing through a column containing 1 mL of Amberlite CG120 (H^+ form) resin, and the column was then washed with 5 mL of water. The combined eluate and washing fluids were evaporated to dryness and derivatized with AMC. For the analysis of sialic acids, a glycoprotein sample was dissolved in 100 μL of 60 mM phosphate buffer (pH 7.0) containing neuraminidase (0.1 U) and *N*-acetylneuraminate pyruvate-lyase (0.1 U), and the mixture was incubated for 5 h at 37°C. After the mixture was heated for 1 min at 100°C, the solution was DI with a column containing 1 mL each of Amberlite CG120 (H^+ form) and CG400 (acetate form) resins, followed by addition of 2 nmol IS.

2.3 Preparation of oligosaccharides from glycoproteins

N-Linked oligosaccharides were prepared from 50 μg of each lyophilized glycoprotein. Each sample was dissolved in 50 μL of 50 mM phosphate buffer (pH 7.9) containing 0.1% SDS and 2% 2-mercaptoethanol. The solution was heated at 100°C for 5 min. After cooling, the solution was mixed with 5 μL of 7.5% NP-40 and 5 mU of peptide-N^4-(acetyl-β-glucosaminyl)-asparagine amidase F, and the reaction mixture incubated for 2 h at 37°C. Deglycosylated proteins were precipitated by the addition of 180 μL of ice-cold ethanol and removed by centrifugation at 10 000 rpm for 5 min. The supernatant was dried using a centrifugal evaporator (Tomy, Tokyo, Japan) and stored in a refrigerator until use.

2.4 Derivatization of saccharides with AMC

Scheme 1 shows the reductive amination reaction of saccharides with AMC. The procedure was described previously [14].
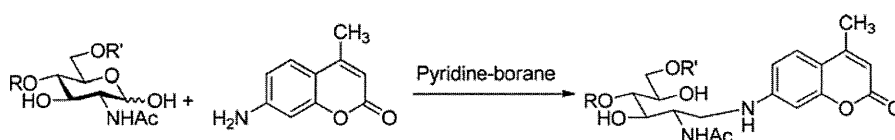
Scheme 1. Reductive animation of a saccharide with AMC as a fluorescent tag.

Briefly, a lyophilized sample containing saccharides (~10 nmol) in a screw-capped polypropylene tube (0.5 mL volume) was mixed with 20 μL of AMC solution (60 mM in DMF) and then mixed with 20 μL of pyridine–borane solution (0.2 M in acetic acid). The solution was then heated at 70°C for 60 min and the reaction terminated by addition of 60 μL of water and chilling of the reaction mixture in an ice bath, followed by evaporation to dryness. The resultant residues were dissolved in 500 μL of 0.5 M acetic acid in aqueous 30% ACN for CE analysis.

2.5 Derivatization of saccharides with AMAC and ABEE

A monosaccharide mixture or isomaltooligosaccharides was labeled according to previously reported methods [16, 17] with slight modification. Each 2.5 μL of 0.3 M AMAC in DMSO/30% acetic acid (7:3, v/v), and 1 M NaBH$_3$CN in DMSO was added to dry saccharide samples (~10 nmol). The solution was incubated at 37°C overnight and the reaction terminated by adding 50 μL of water–methanol (1:1, v/v).

A 20 μL portion of ABEE solution (1 mmol of ABEE and 35 mg of NaBH$_3$CN, and 41 μL of acetic acid dissolved in 350 μL of methanol) was added to a saccharide sample (~100 nmole), and the solution was heated at 80°C for 1 h. The resultant solution was dried and dissolved in 100 μL of water–methanol (9:1, v/v). Excess ABEE, immiscible in the solvent, was removed by centrifugation, and the supernatant was used for the CE analysis.

2.6 Instrumentation for CE analysis

Apart from a reference experiment using a bare fused silica capillary (50 μm id) for Fig. 1A, PDMS-coated capillaries (InertCap I®; GL Sciences, Tokyo, Japan) of 50 μm id with an effective length of 40 cm (50 cm in total) were used, with a 1:9, v/v, mixture of ACN and borate buffer containing 0.05% hydroxypropylcellulose as a BGE; 200 mM sodium borate (pH 9.5) for monosaccharide analysis and 250 mM potassium borate (pH 9.0), and 100 mM Tris borate (pH 8.5) for neutral and acidic oligosaccharide separation, respectively. A P/ACE MDQ CE system (Beckman Coulter, Brea, CA, USA) was used. An LED light (LLS-365, Ocean Photonics) as a source of 365 nm light was connected with an optical fiber (P600-2-UV/Vis, Ocean Photonics), and the fluorescence due to AMC derivatives was detected by passing through a 420 nm band path filter. The capillary was thermostated at 25°C. Sample

solution was injected for 5 s by application of pressure of 3.45 kPa. Separation was conducted by application of −15 kV. After each run, the capillary was washed by introducing a buffer solution from the outlet of the capillary using pressure (34.5 kPa, 2 min). AMAC derivatives were detected fluorometrically using an argon laser (488 nm) and the optical system for the fluorescein detection. ABEE derivatives were detected based on absorbance at 312 nm. Other conditions were the same as those for AMC derivatives.

The volume of sample solution injected into the capillary was not certain. Here we chose the following calculation to estimate injected amount of sample in sample solution:

$$V = \frac{\Delta P d^4 \pi t}{128 \eta L}$$

where V is the volume in m^3 delivered across the capillary, ΔP denotes the pressure drop across the capillary (Pa), d signifies the internal diameter of the capillary (m), t is the duration of pressure application (s), η represents the buffer viscosity (Pa·s), and L is the total capillary length (m).

3 Results and discussion

3.1 Optimization of separation conditions

Alkaline borate buffer has often been used in CE separation of mixtures of monosaccharide derivatives [18]. Borate forms complexes with polyalcohols, including saccharide derivatives in solution, and the borate–polyalcohol complexes possess negative charges, which are forced to move toward the anode in an electric field. Stability and negativity of the saccharide–borate complex depend on the configuration of adjacent hydroxyl groups (i.e., the type of monosaccharide). Moreover, the pH and concentration of borate buffer influence the formation of polyoxy acid with borate ions as well as the complex formation, and therefore also affect the mobility of borate–polyol complexes [19]. Most reports on CE of monosaccharide derivatives using alkaline borate buffer were performed using a bare fused silica capillary. Under such conditions, monosaccharide derivatives travel from anode to cathode because of strong EOF, and separate as anions, based on the molecular size and stability of the borate complexes. Moreover, a large amount of excess fluorescent reagents also travels to the cathode, which may cause deviations in migration times and heavy drift of baselines.

Here, we used a PDMS-coated capillary instead of a bare fused silica capillary to suppress EOF and to specifically move acidic borate–saccharide complexes toward the anode. Reductive amination of carbohydrates with primary amines generates secondary amine derivatives of linear polyalcohols (i.e.,
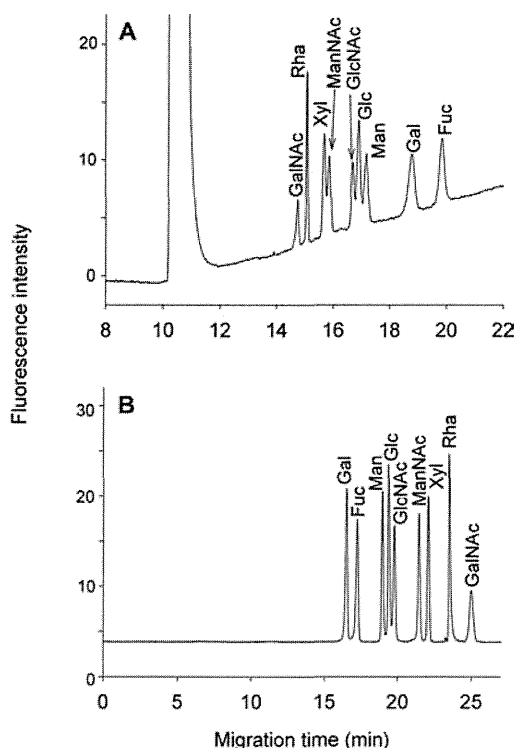
Figure 1. Fluorescent CE analysis of selected monosaccharides in borate complexation mode using a bare fused silica capillary (A) and a PDMS-coated capillary (B). Analytical conditions: BGE, ACN and 200 mM sodium borate (pH 9.5) containing 0.05% hydroxypropylcellulose (1:9, v/v); capillary size, 50 μm id × 50 cm (40 cm for detector); capillary temperature, 25°C; applied voltage +15 kV (A) and −15 kV (B); detection, fluorescence with 365 nm LED.

aminoalditols). Excess aromatic amines and their decomposition products residing in the reaction mixture cannot be charged in alkaline borate buffer. In contrast, monosaccharide derivatives having linear polyalcohol structures easily generate negative charges as borate complexes, which move toward the anode in an electric field. Therefore, the excess reagents in the reaction mixture can be removed from electropherograms without requiring purification before analysis.

Figure 1A shows the separation of AMC derivatives of monosaccharides obtained by reaction on positive mode separation using a bare capillary and alkaline borate buffer as BGE. Reaction products of AMC-labeled derivatives show an intense, tailing signal of excess AMC at 11 min and baseline drift, which could not be removed by addition of surfactants to the BGEs. In contrast, a combination of negative separation mode using 200 mM borate buffer containing 0.05% hydroxypropylcellulose and PDMS-coated capillary, as shown in Fig. 1B, suppressed the generation of EOF and therefore induced the movement of anionic borate complexes to the anode. This enables specific detection of saccharide derivatives. Addition of ACN prevents the precipitation of excess reagent. Therefore, the electropherogram comprised peaks corresponding to monosaccharide derivatives, with no peaks

because of excess reagent. This result indicates the usefulness of the separation conditions.

3.2 Monosaccharide analysis

We previously reported that the use of pyridine-borane rather than the sodium cyanoborohydride normally used enables quantitative derivatization of all component monosaccharides in glycoproteins [14]. Here, we optimized the separation conditions of AMC-labeled monosaccharides containing excess reagents using CE with fluorometric detection by LED.

The resolution between AMC monosaccharide derivatives depends strongly on the pH of the borate buffer and also the species and concentration of organic solvent. Resolution of Man-Glc-GlcNAc and ManNAc-Xyl is invariant with pH but the separation window (i.e., time window for separation of monosaccharides) is broadened with increasing electrophoresis buffer pH. The concentration of the borate buffer mainly affects the peak shape of AMC derivatives. With increasing buffer concentration, the sharpness of AMC monosaccharide peaks increased, reaching a maximum of over 200 mM. The higher concentration causes Joule heating because of the increase in electric current. Addition of a water-miscible solvent such as methanol, ethanol, or ACN is essential to prepare a clear solution from the AMC reaction mixture because of the low solubility of AMC in water. Among these three solvents, we found that the addition of ACN enhanced the resolution of fucose from other monosaccharide derivatives. Baseline resolution was obtained using a 1:9 v/v mixture of ACN and borate buffer containing 0.05% hydroxypropylcellulose. However, the anions residing in the reaction mixture partly diminished the sharpness of specific peaks. To enhance the sharpness of saccharide peaks, acetic acid was added to AMC-labeled sample at a concentration of 0.5 M. Good resolution between the nine monosaccharide derivatives was obtained under the optimized conditions, as shown in Fig. 1B.

3.3 Analysis of component monosaccharides in glycoproteins

The optimized conditions were applied to the analysis of component monosaccharides in a number of glycoproteins. Saccharide chains in glycoproteins comprise Man, Gal, Fuc, GlcNAc, GalNAc, NeuAc, and NeuGc. Before the analysis, the linearity range and lower LOD were examined. As shown in Fig. 2, linear quantitation ranges were obtained over the concentration range between at least 0.4 and 400 μM (calculated to be 140 amol to 140 fmol). Figure 3 shows the separation of 4, 0.4, and 0.04 μM mixture. Apparently, 4 and 0.4 μM are within the quantitation range, but the concentration of 0.04 μM were apparently below the detection limit, for example, peak height of Rha is only 2.5 times of noise. Therefore we determined 80 nM (ca. 28 amol) as the LOD (S/N = 5). The hydrolytic conditions required for quantitative
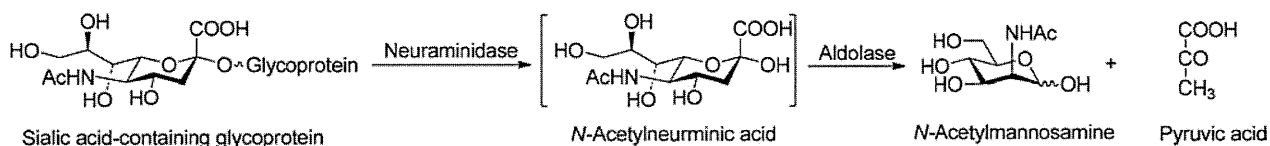
Scheme 2. Enzymatic conversion of sialic acids in glycoproteins to mannosamine derivatives.
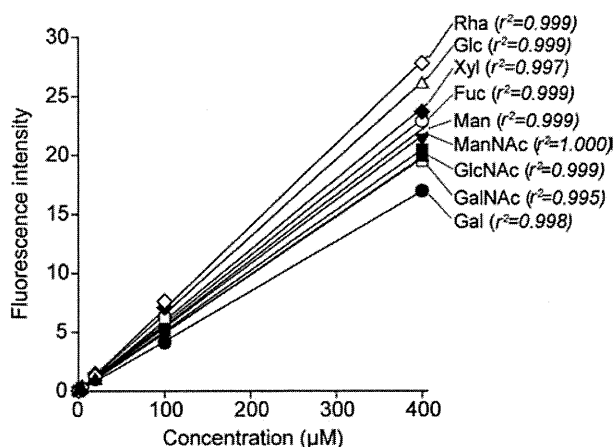

Figure 2. Calibration plots for quantitation of nine saccharides as AMC derivatives.

recovery of monosaccharides vary depending on the type of monosaccharides [20]. Therefore, we used different conditions for neutral aldoses, hexosamines, and sialic acids. Two molar TFA was chosen for hydrolysis of neutral aldoses, including Fuc, Gal, and Man, while 4 M hydrochloric acid was used for the release of hexosamines. Hydrolysis was performed at 100°C for 6 h. In contrast sialic acids are easily decomposed in strong acids so we chose enzymatic release and the generated neuraminic acids were further converted to N-acetyl- or N-glycolylmannosamine derivatives by the action of aldolase (N-acetylneuraminate pyruvate-lyase, EC 4.1.3.3), as shown in Scheme 2 [15]. Therefore, the contents of both types of neuraminic acid could be estimated from the peak areas of corresponding mannosamine derivatives, appearing at 17.5 and 18.5 min, respectively.

Figure 4 indicates the results of monosaccharide analysis of several glycoprotein samples. Rha was chosen as a common IS for the analysis. Acid glycoprotein, fetuin, ovalbumin,

ribonuclease B, and transferrin were chosen as common glycoproteins, and BSM was used for sialic acid analysis because mucin contains high concentrations of NeuAc and NeuGc. Carbohydrate chains of acid glycoprotein and transferrin are composed of complex oligosaccharides, whose chains consist of GlcNAc, Man, Gal, Fuc, and NeuAc [21, 22]. Electropherograms clearly indicated the presence of these monosaccharides. The fucose content of transferrin is low but the electropherogram clearly indicated the presence of Fuc in the hydrolysates of transferrin. Fetuin contains both N- and O-linked glycans [23–25]. Therefore, the oligosaccharide chains are composed of GlcNAc, GalNAc, Man, Gal, and neuraminic acids. These monosaccharides appeared in the electropherograms. Moreover, a small peak of N-glycolylmannosamine indicates the presence of NeuGc in this glycoprotein, at a level one order lower than that of NeuAc. Ovalbumin comprises high-mannose type and a series of hybrid-type glycans, which implies the presence of GlcNAc, Man, and a small quantity of Gal [26–28]. RNB comprises a series of high-mannose type oligosaccharides [29]. Therefore, hydrolysates include only Man and GlcNAc. These monosaccharides appeared in electropherograms.

Based on the peak area of each sample relative to IS, the monosaccharide contents were estimated and are summarized in Table 1. The results were compared to those of previously reported data [15, 30]. The accuracy of the present method involving the hydrolysis process could not be fully evaluated by comparison with previous data as contents of fucose in acid glycoprotein, Man in fetuin, and GlcNAc and neuraminic acids in transferrin were apparently lower than the reported values. In contrast, Man in ribonuclease and hexosamines in fetuin were at higher levels than previously reported. The sialic acid contents of BSM were three times higher than those of reported values, which should be due to difference in commercial preparation. We believe the removal of the purification step for derivatives could enhance the
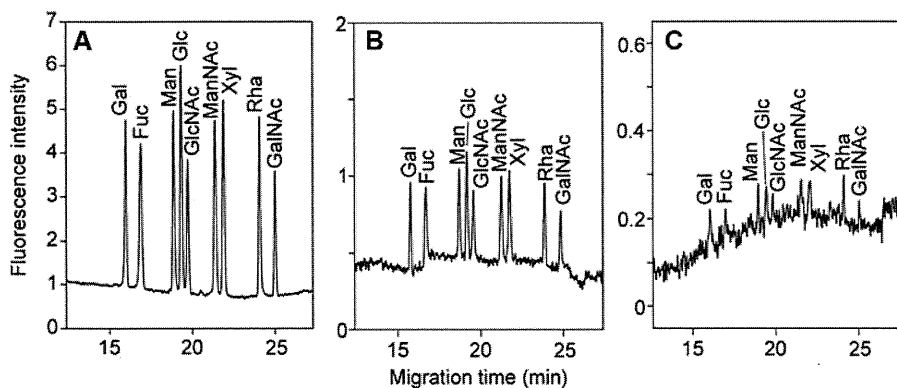
Figure 3. CE analysis of nine saccharides at concentrations of 4 μM (A), 0.4 μM (B), and 0.04 μM (C). Analytical conditions were the same as those used for Fig. 1B.